

## Environmental Research Letters



## LETTER

## The warm Blob in the northeast Pacific—the bridge leading to the 2015/16 El Niño

## OPEN ACCESS

## RECEIVED

23 November 2016

## REVISED

7 March 2017

## ACCEPTED FOR PUBLICATION

20 March 2017

## PUBLISHED

19 May 2017

Original content from this work may be used under the terms of the [Creative Commons Attribution 3.0 licence](#).

Any further distribution of this work must maintain attribution to the author(s) and the title of the work, journal citation and DOI.

Yu-Heng Tseng,<sup>1,6</sup> Ruiqiang Ding<sup>2,3</sup> and Xiao-meng Huang<sup>4,5,6</sup><sup>1</sup> Institute of Oceanography, National Taiwan University, Taipei 10617, Republic of China<sup>2</sup> State Key Laboratory of Numerical Modeling for Atmospheric Sciences and Geophysical Fluid Dynamics (LASG), Institute of Atmospheric Physics, Chinese Academy of Sciences, Beijing 100029, People's Republic of China<sup>3</sup> Plateau Atmosphere and Environmental Key Laboratory of Sichuan Province, Chengdu University of Information Technology, Chengdu 610225, People's Republic of China<sup>4</sup> Ministry of Education Key Laboratory for Earth System Modeling, and Department of Earth System Science, Tsinghua University, Beijing 100084, People's Republic of China<sup>5</sup> Laboratory for Regional Oceanography and Numerical Modeling, Qingdao National Laboratory for Marine Science and Technology, Qingdao 266237, People's Republic of China<sup>6</sup> Authors to whom any correspondence should be addressed.E-mail: [tsengyh@ntu.edu.tw](mailto:tsengyh@ntu.edu.tw), [hxm@tsinghua.edu.cn](mailto:hxm@tsinghua.edu.cn)**Keywords:** Blob, ENSO, North Pacific Oscillation, Victoria modeSupplementary material for this article is available [online](#)**Abstract**

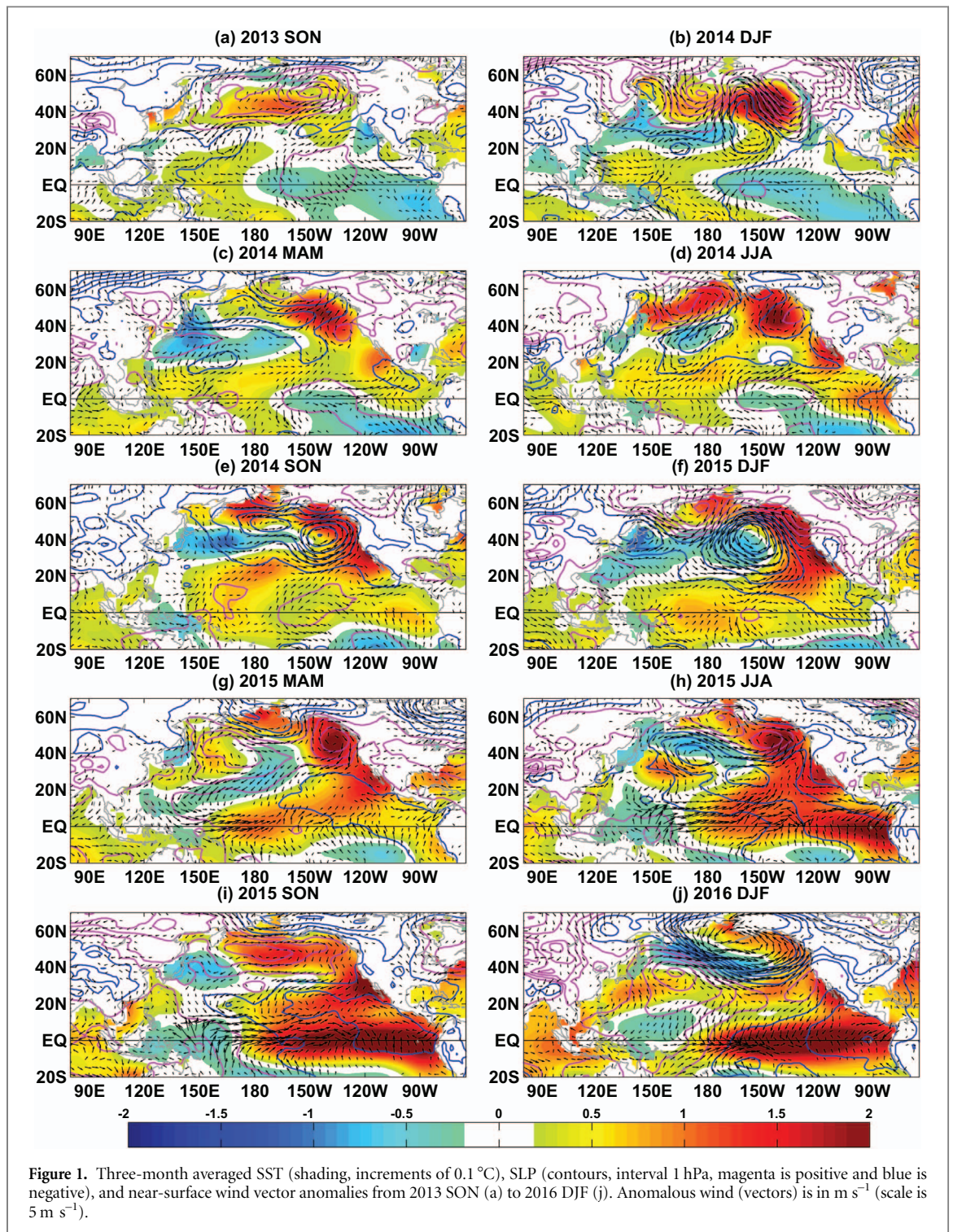
We address the occurrence of the warm anomaly, known as the Blob, that developed from late 2013 to 2015 in the northeast Pacific and its connection with the El Niño–Southern Oscillation (ENSO) variability. The warm Blob results from the enhanced second ocean–atmosphere (O–A) coupled mode of variability in the tropical and North Pacific, representing a small part of the Victoria mode (VM) in the northeast Pacific forced by the strengthened North Pacific Oscillation-like atmospheric pattern since 2013. We also show that this second O–A mode reflects the meridional variability through the tropical–extratropical teleconnection and is an important precursor to the ENSO variability. The process is confirmed by the coupled patterns that evolved from late 2013 to 2016 and the multi-year persistence of the warm Blob. We emphasize the role of evolving basin-scale VM but not the warm Blob itself prior to the ENSO variability. Hence, the Blob and the most recent 2015/16 El Niño, which differs significantly from the other large El Niños in terms of the triggering hemisphere, are actually linked rather than independent phenomena.

**1. Introduction**

An extremely warm sea surface temperature (SST) event developed in the northeast Pacific in late 2013. The warm SST anomaly, which became popularly known as 'the Blob', reached temperatures more than 2.5 °C higher than the climatological mean SST in a few extratropical regions of the North Pacific (Bond *et al* 2015) and was prominent in the south of the Gulf of Alaska (figure 1). The warm Blob has attracted much attention. Bond *et al* (2015) attributed the development of the Blob to strongly positive sea level pressure (SLP) anomalies over the Gulf of Alaska that suppress the local ocean heat loss in the atmosphere. As we will show later, the mechanism described resembles the typical ocean response to the strengthened northern lobe of the

North Pacific Oscillation/West Pacific Pattern (NPO/WP) (Linkin and Nigam 2008, Baxter and Nigam 2015) over the northeast Pacific.

From early 2014, the North Pacific gradually developed a spatial pattern with negative SST anomalies extending from the subtropical western Pacific to the central North Pacific encircled by warm SST anomalies around the North Pacific coast that reach the central tropical Pacific and the western Bering Sea (see the evolution of three-month averaged SST, SLP, and surface wind anomalies in figure 1). This SST distribution resembles the spatial pattern of the Victoria mode (VM), which is a basin-scale pattern combining the active roles from both the western (cold) and eastern (warm) North Pacific (Bond *et al* 2003, Ding *et al* 2015a, Ding *et al* 2015b). The eastern



part of the basin-scale VM is commonly known as the Pacific meridional mode (PMM; Chiang and Vimont 2004, Chang *et al* 2007) or North Pacific gyre circulation (NPGO; Di Lorenzo *et al* 2008, Di Lorenzo *et al* 2015). The major differences between the VM and PMM/NPGO are described by Ding *et al* (2015a) and we use the VM in this paper to emphasize the important basin-scale changes instead of the regional response. A neutral to weak El Niño condition developed at the end of 2014 (Levine and McPhaden 2016). The heat content and SST anomalies in the tropical Pacific continuously evolved into a strong El

Niño after April 2015 that reached its mature phase at the end of 2015 due to the phase locking to the seasonal cycle. Hereafter, we refer to the most recent strong El Niño event, starting from the end of 2014 and lasting to early 2016, as the 2015/16 El Niño (a single event). Based on the SST data, the 2015/16 El Niño surpassed the 1997/98 El Niño, making it one of the strongest El Niño events on record (e.g. more than  $3^{\circ}\text{C}$  warmer than the climatological mean in the Niño 3.4 region).

There are many questions about the two extremely warm SST events in the extratropical and tropical

Pacific, particularly regarding their causes, interactions, and associated climate impacts. Most researchers believe there is no connection between these two extreme events, while both could have affected the recent drought in the west of the USA (e.g. Jacox *et al* 2016, Amaya *et al* 2016). Feng *et al* (2014) argued that the SST anomalies off the coast of Baja California could act as a possible precursor of ENSO through the PMM dynamics. However, conclusions regarding the impacts of the Blob on the weather (e.g. Bond *et al* 2015, Hartmann 2015) and how the strong El Niño and the strong Blob are linked should be drawn with caution because of the complicated ocean–atmosphere (O–A) interaction in the North Pacific. Di Lorenzo and Mantua (2016) recently confirmed that the tropical–extratropical teleconnection in 2014 has played a key role in maintaining the multi-year persistence of the North Pacific atmosphere since late 2013, but they have not addressed the relationship between the Blob and the 2015/16 El Niño yet. Also, no study has discussed the major differences between the 2015/16 El Niño comparing with the previous strong El Niños (e.g. 1982/83, 1997/98). Here we aim to explicitly show that this warm Blob is actually the northeast signature of the evolving VM in the North Pacific (gradually enhanced after 2013 and weakened in 2016), leading to the mature/decay of 2015/16 El Niño. It is the typical ocean expression of the second dominant O–A coupled mode in the North Pacific, primarily forced by the NPO-like atmospheric pattern. Most importantly, our results confirm that the phase change of the second O–A coupled mode actually leads to the ENSO variation a few seasons later through the evolution of the VM (Ding *et al* 2015a, 2015b). Therefore, the warm Blob is a clear precursor to (but not a direct cause of) the development of the 2015/16 El Niño, representing the typical extratropical impact from the Northern Hemisphere (NH). The warm Blob and 2015/16 El Niño are closely linked rather than independent phenomena.

## 2. Methods

### 2.1. Observational data

We used NOAA extended reconstructed sea surface temperature (ERSST) V4 data (Huang *et al* 2015) and the National Centers for Environmental Prediction–National Center for Atmospheric Research (NCEP–NCAR) reanalysis (Kistler *et al* 2001) to compute the Combined Empirical Orthogonal Function (CEOF) after removing the monthly mean climatology and the linear trend from the monthly data for 1958–2016. This period was chosen to minimize the impact of limited observational data before 1960 while maintaining sufficient effective samples to ensure statistical significance. All correlations and color figures with shading in this paper are significant at the  $p < 0.05$  level. The effective degrees of freedom are determined

using the method recommended by Bretherton *et al* (1999). The same results can be obtained when different time periods and different datasets are examined (e.g. Hadley Centre SST and SLP2 dataset and ERA-interim since 1979). The covariability between SLP and SST anomalies is analyzed because it can better explain the O–A dynamical links in the Pacific. The study area ( $20^{\circ}\text{S}$ – $70^{\circ}\text{N}$  and  $80^{\circ}\text{E}$ – $65^{\circ}\text{W}$ ) covers the tropical and North Pacific. A three-month average is applied for all time series used here.

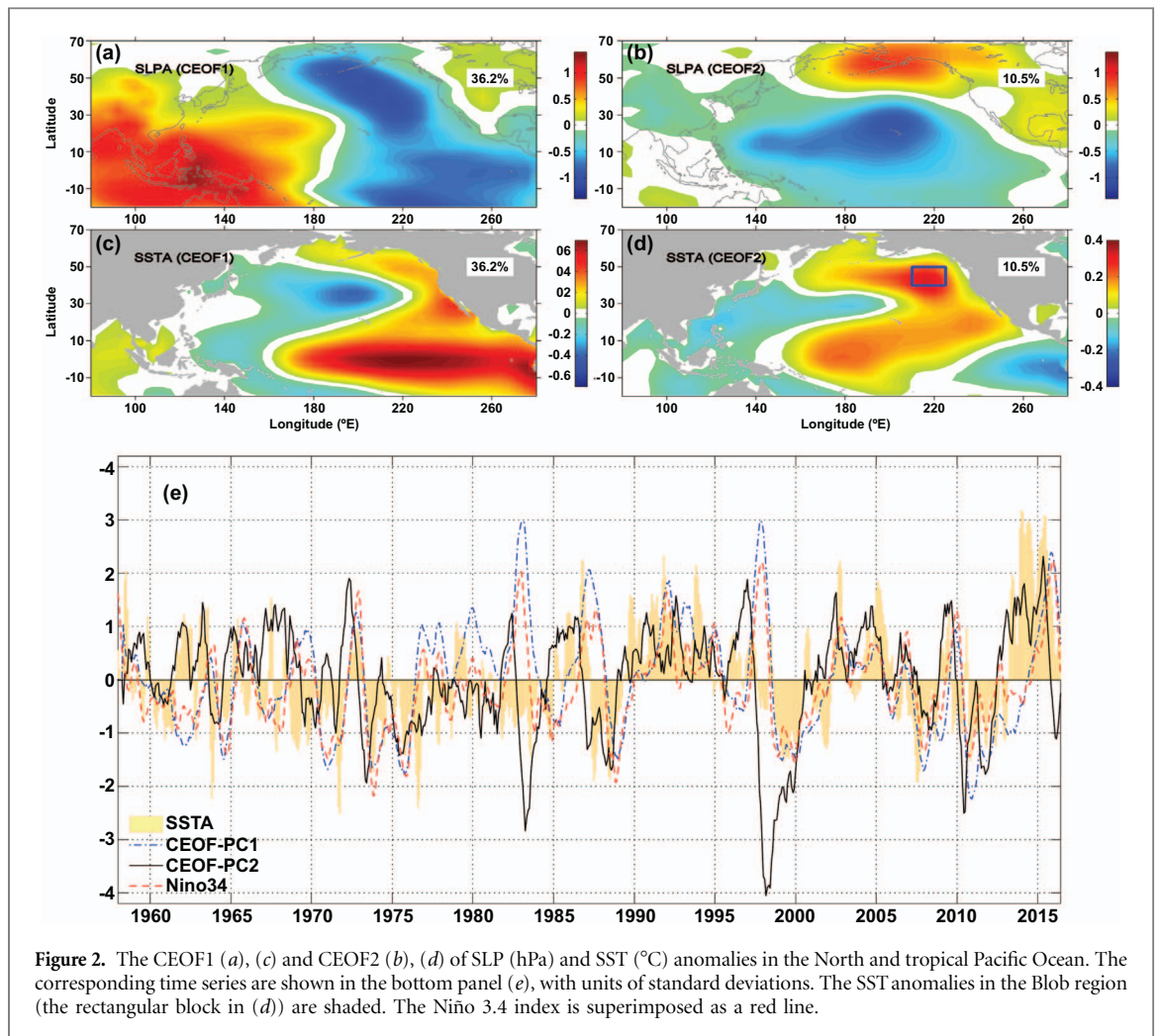
To emphasize the large-scale pattern and the evolution variability, a three-month low-pass and  $4^{\circ} \times 4^{\circ}$  spatial Blackman-window filter is applied to the monthly SLP and SST anomaly fields for the CEOF. Before computing the CEOF, both anomaly fields are normalized by the domain average standard deviations. Hereafter, seasons refer to those of the NH.

### 2.2. Community Earth System Model large ensembles (CESM-LENS)

To further support the relation between the two dominant O–A modes, we also analyze the historical simulations from the large ensembles (LENS) of CESM version 1.1 (Kay *et al* 2015). The LENS are forced with historical greenhouse gases and aerosol emissions from 1920 to 2005. These ensembles only differ in their 1920 initial conditions at the round-off error level (Kay *et al* 2015). Since all ensemble members show very similar results, we only present the control simulation here from 1850–2005 to emphasize the robust feature.

## 3. Results

In order to demonstrate that the warm Blob is indeed the SST signature of the second coupled O–A mode in the northeast Pacific, we first show the two leading CEOF modes and their corresponding time series of principal components (PCs) in figure 2. The variances of the leading (CEO1) and second (CEO2) CEOFs are 36.2% and 10.5%, respectively. The third mode (8.6% variance) is not addressed here because it is irrelevant to our discussion. The CEO1 of the SLP anomalies in the Pacific (figure 2(a)) shows mainly the Aleutian Low (AL), the semi-permanent low pressure winter center over the Aleutian Islands caused by planetary waves, in association with the typical Southern Oscillation dipole near the tropics (a strong western Pacific subtropical high and the other strong pressure low near the eastern tropics). They are the typical atmospheric expressions accompanying Pacific Decadal Oscillation (PDO) and El Niño–Southern Oscillation (ENSO) patterns. This canonical PDO/ENSO pattern also emerges in the CEO1 of the SST anomalies (figure 2(c)), with warm anomalies in the cold tongue from the central–eastern tropical Pacific and cold anomalies in the western Pacific, which extend to the central North Pacific in the mid-latitudes.



Furthermore, the temporal evolution of PC1 is strongly correlated with the Niño 3.4 index (correlation coefficient  $R = 0.88$ ; time series compared in figure 2 (e)) and is moderately correlated with the PDO index ( $R = 0.67$ ). Therefore, we can conclude that the spatial pattern of CEOF1 and its PC1 approximately correspond to the ENSO variability and the persistent teleconnection with the PDO through the atmospheric bridge (Zhang *et al* 1997, Newman *et al* 2016, Di Lorenzo and Mantua 2016).

The CEOF2 of the SLP anomalies in the North Pacific (figure 2(b)) presents the typical meridional dipole structure of the NPO in the central–eastern Pacific, with positive anomalies north of  $45^{\circ}\text{N}$  over the Aleutian Islands and negative anomalies in the south between  $0^{\circ}$  and  $40^{\circ}\text{N}$  (over Hawaii). This NPO pattern is very similar to that reported previously (Linkin and Nigam 2008, Furtado *et al* 2012) and is a robust winter atmospheric feature. In addition, the associated SST footprint resembles the VM described previously (Bond *et al* 2003, Di Lorenzo *et al* 2008, Ding *et al* 2015a) (figure 2(d)). In particular, the geographical location of the largest variance is approximately consistent with the Blob location reported in Bond *et al* (2015) (the rectangular box in figure 2(d):  $40\text{--}50^{\circ}\text{N}$ ,  $135\text{--}150^{\circ}\text{W}$ ).

This consistency suggests that the Blob is the SST signature of the CEOF2 in the northeast Pacific. Spatially, the SST anomalies shown in early 2014 (figures 1(b) and (c)) qualitatively resemble figure 2(d) in the central to eastern Pacific. In winter 2013/14 (figure 1(b)), the SLP anomalies show a clear quasi-meridional dipole with low/high SLP anomalies at south/north in the extratropical region, similar to the NPO dipole in figure 2(b), but have a much larger variation; see Baxter and Nigam (2015) for further discussion of the 2013/14 NPO pattern. The spatial pattern had evolved into the CEOF1-like pattern by the end of 2014 (the AL and the subtropical high in the SLP anomalies with PDO/ENSO pattern in the SST anomalies; see figure 1(f)). But the subtropical high in the western Pacific is not very intense with a weak zonal dipole in the tropics, suggesting a very weak El Niño like phenomena (Central Pacific warming signature, see Tseng *et al* 2017). In the extratropical Pacific, we can still observe a similar meridional dipole of SLP anomalies with an enhanced southern pole (i.e. enhanced AL) in winter 2014/15. As we mentioned earlier, the meridional dipole can enhance the Pacific VM pattern in spring which can favor the development of ENSO. Therefore, we can see the evident VM pattern in spring 2015 (figure 1(g)). This VM pattern

is much stronger in 2015 than 2014 (comparing figures 1(c) and (g), particularly the tropical and subtropical signatures), showing the enhanced ENSO-favorable SST pattern.

Then, the typical CEOF1 pattern is further strengthened in summer 2015 (figure 1(h)) and becomes robust and prominent at the end of 2015 (figure 1(i)), leading to the mature phase of the 2015/16 El Niño (figure 1(j)). The growth of CEOF1 can be seen by the significant increase of PC1 during the whole of 2015 (figure 2(e)), consistent with the development of PDO in 2015 (Di Lorenzo and Mantua 2016). The subtropical high in the western Pacific is now completely developed (figure 1(j)).

The above results confirm the positive CEOF2 is a robust feature in the North Pacific from early 2014 to 2015. Winter 2014/15 shows the existence of a meridional NPO-like pattern in the extratropical Pacific and a zonal ENSO-like pattern in the tropical and subtropical Pacific, suggesting the transition phase of ENSO. Figure 3(a) further shows the lead-lag correlations between the time series of PCs associated with the first two CEOF modes (also Niño 3.4) and SST anomalies in the Blob region defined by Bond *et al* (2015) (95% confidence levels are shown as dotted lines). The SST anomalies in the Blob region lag PC2 by four months ( $R = 0.54$ ) and lead the Niño 3.4 by five months ( $R = 0.43$ ) (also PC1 by seven months,  $R = 0.41$ ). The lead of PC2 relative to the SST anomalies in the Blob region can be directly seen in the respective time series shown in figure 2(e) (e.g. the black line becomes positive a few months earlier than the shading in 2012–2013). The relation is very robust even if we use data prior to 2014 (see figure S1 available at [stacks.iop.org/ERL/12/054019/mmedia](http://stacks.iop.org/ERL/12/054019/mmedia) for the lead-lag correlation during 1958–2011). Both of the SST anomalies in the Blob region and the PC2 show large-amplitude variations associated with the warming VM pattern that started in 2013 (the largest magnitude since 1958). The second positive peak of PC2 is January 1997, which was followed by the 1997/98 El Niño. The similarity between the winter 2013/14 SST/SLP patterns and the typical NPO/VM, combined with the correlation between PC2 and the SST anomalies in the Blob, confirms that the unusually warm temperatures in the northeast Pacific that prevailed from late 2013 to 2015 are actually the typical extratropical signature of the VM (Ding *et al* 2015a, Ding *et al* 2015b), which is inherent in the second O–A coupled mode of variability in the North Pacific.

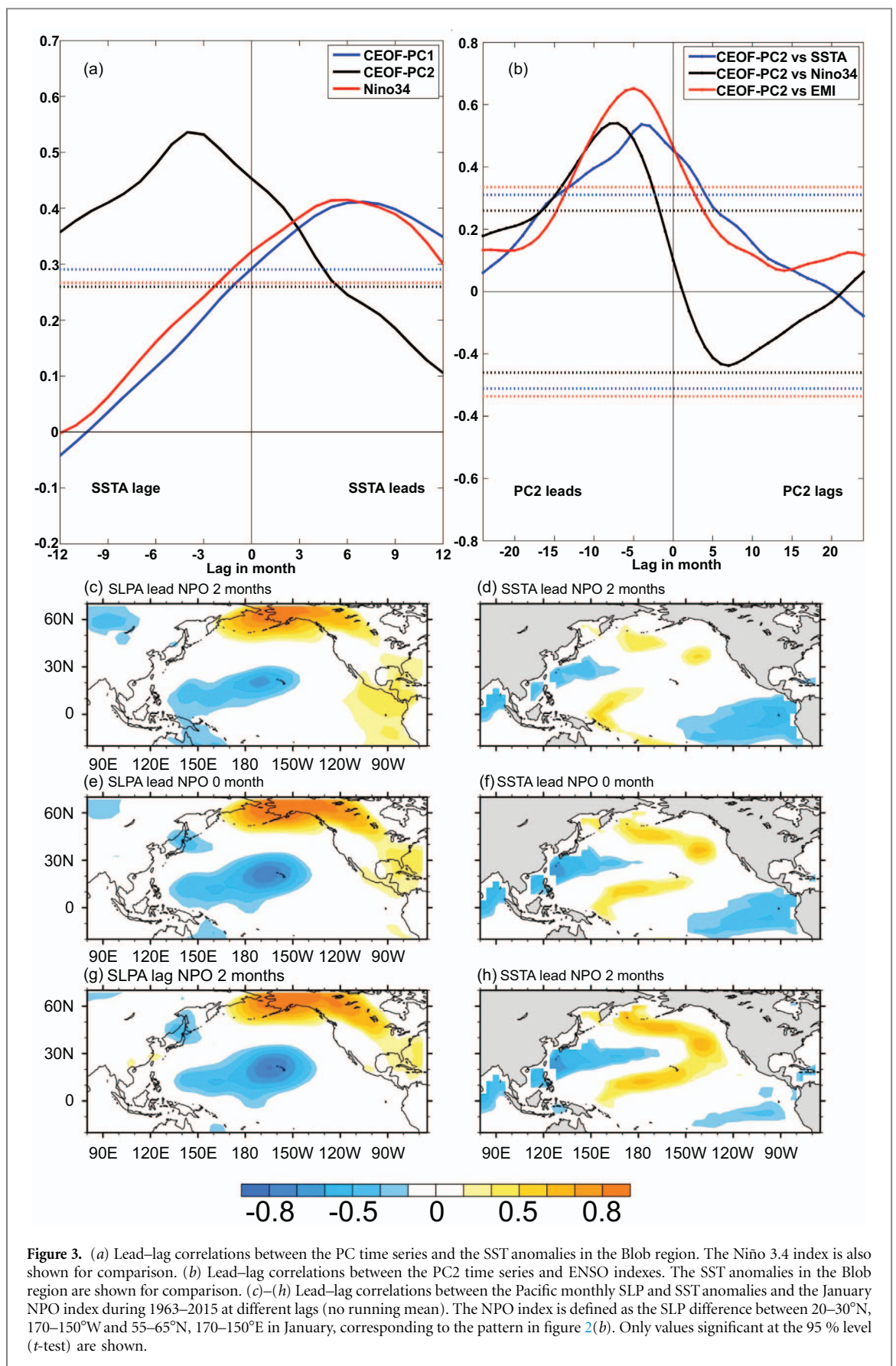
We next establish the connection between the CEOF2 and the ENSO variation. Figure 3(b) shows the lead-lag correlations between PC2 and two different ENSO indices (the Niño 3.4 index and the El Niño Modoki index (EMI), defined by Ashok *et al* (2007)). The similar correlation between PC2 and the SST anomalies over the Blob region is also shown for comparison. It is evident that PC2 consistently leads the Niño 3.4 and EMI ( $R = 0.55$  and  $0.68$ , respectively)

with slightly different lags. These results confirm that the appearance of the CEOF2 prior to ENSO occurrence (Furtado *et al* 2012) and the spatial pattern of CEOF2 can potentially be seen as precursors of ENSO. In general, PC1 and the Niño 3.4 index are almost in phase, but the CEOF2 pattern associated with PC2 can last several months (approximately 6–10) before PC1 matures. A similar lead of PC2 also applies to the termination of ENSO. A large phase change of the CEOF2 can be found clearly a few months before the termination of ENSO in many large events (e.g. 1972/73, 1982/83, 1997/98, 2015/16 El Niños and 1973/74, 1988/89, 1998/99 La Niñas), see figure 2(e).

We further list all medium to strong ENSO events (total 18 El Niños and La Niñas) after 1965 in table 1. 83% of the ENSO events (15 out of 18) are associated with large SST anomalies in the warm Blobs more than nine months in advance (bold: larger than one standard deviation). These strong evidences indicate that the SST anomalies of the Blob (with shorter lag time than the two ENSO indices) may be a bridge between the first two dominant coupled modes and, specifically, an SST expression of the CEOF2 pattern of NPO/VM leading to the CEOF1 pattern of PDO/ENSO. The evolution can be further seen in the correlation between the Pacific SST anomalies and the January Niño 4 index at different lags during the period 1958–2010 (figure S2 in the supporting information; the CEOF1 SST pattern is similar to figure S2(f) and the CEOF2 SST pattern is similar to figure S2(c)).

These results are consistent when the HadSST and the HadSLP2 are used to represent the coupled O–A mode (figure S3). The spatial patterns of the first two coupled models and their variances are quite similar. Although the maximum correlations are slightly lower using the HadSST/HadSLP2 data, the leading role of CEOF2 (associated with the SST anomalies' variability in the Blob region) in the ENSO variability is still significant at the expected timing. The correlation is always better if the NCEP data is used instead of HadSLP2 regardless of SST observations. The linkage between the CEOF1 and CEOF2 can be better represented in the O–A coupled climate model. Figure 4 shows the two dominant CEOF patterns and the lead-lag correlation based on the control simulation of CESM-LENS during 1850–2005. The described connection between the CEOF2 and the ENSO variation is quite robust with correlation above 0.55 regardless of ENSO types. In fact, all CESM-LENS simulations show such a strong relationship between the PC2 of the CEOF2 and the ENSO with minor differences in the variance and pattern, supporting the close lead-lag relation between the first two dominant modes (see figure S4 for the selected CESM-LENS simulations and also the discussion in Deser *et al* 2012).

Several studies have indicated that the CEOF2 responds to the atmospheric forcing of the NPO.



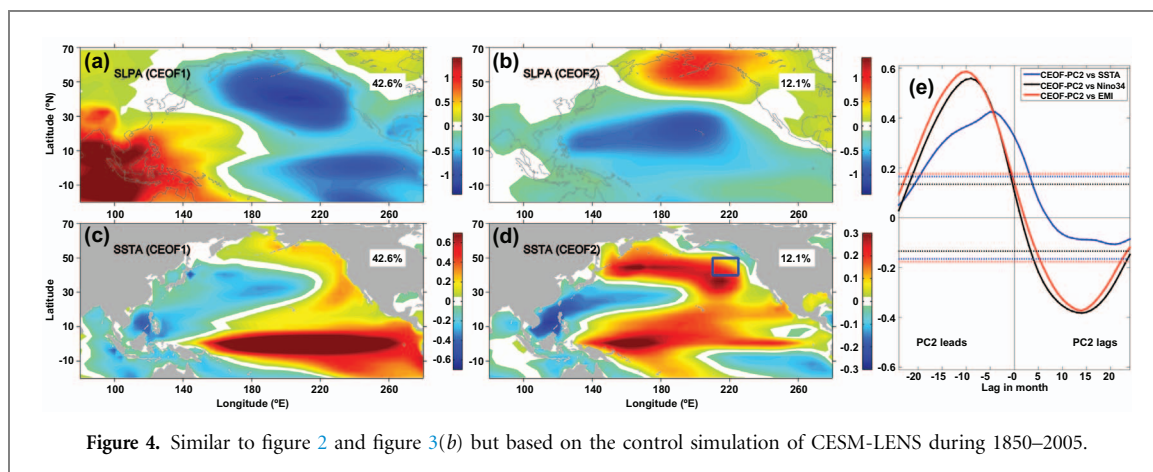
Ding *et al* (2015a) suggested that the VM might act as an effective pathway for NPO-like atmospheric variability to drive ENSO variability via the seasonal footprinting mechanism (SFM) (Vimont *et al* 2003).

The warm Blob that developed after late 2013 (figure 1) is actually the northeast part of the VM and was actively involved in the dynamical process that evolved into the 2015/16 El Niño. The evolving

**Table 1.** Medium to strong ENSO events after 1965 defined by CPC<sup>a</sup> (the SST anomalies in the Blob region larger than one standard deviation preceding the ENSO events are labeled in bold).

El Niño	1965/66, 1972/73, 1982/83, 1986/87, 1987/88, 1991/92, 1997/98, 2002/03, 2009/10, 2015/16
La Niña	1970/71, 1973/74, 1975/76, 1988/89, 1998/99, 1999/00, 2007/08, 2010/11

<sup>a</sup> [www.cpc.ncep.noaa.gov/products/analysis\\_monitoring/ensostuff/ensoyears.shtml](http://www.cpc.ncep.noaa.gov/products/analysis_monitoring/ensostuff/ensoyears.shtml)



SST and SLP anomalies in figure 1 confirm the detailed mechanism described by Ding *et al* (2015a) (e.g. the similarity between figures 1(a)–(c) and the correlation maps in their figures 7(a)–(c), although with a slightly different southern lobe of the NPO), who suggested that a large warm Blob might effectively lead to a strong El Niño. However, the Blob is not the cause of 2015/16 El Niño. Rather, it is a basin-scale transition process bridging the extratropical forcing and ENSO variation. The reduced net surface heat fluxes shown in winter 2013/14 (Bond *et al* 2015) are consistent with the NPO forcing on the VM and previous winter studies in the North Pacific. After the VM reaches the mature phase in March 2014 (with a band of significant SST anomalies in the subtropical central to eastern North Pacific) with a decreasing atmospheric impact, the coupled positive wind–evaporation–SST feedback becomes active, contributing to subsequent equatorward development of warm SST anomalies in the central–eastern Pacific as the ENSO develops (Ding *et al* (2015a), see also figure 10 in Tseng *et al* (2017) and its associated discussion on the tropical evolution in 2014). This warming enhances the SST zonal gradient across the tropical Pacific, thus forcing the anomalous southwesterlies in the western tropical Pacific (figure 1) from spring to summer 2014. The evolution of the SST anomalies in the northeast Pacific is consistent with the surface heat flux changes discussed previously (e.g. Ding *et al* 2015a) and the characteristics of the evolved SFM (Vimont *et al* 2003).

To verify that the warm Blob that developed after late 2013 is not a unique event but a direct and strong NPO footprint commonly seen in the northeastern Pacific before the El Niño, we further illustrate lead–lag correlations between the Pacific SLP and SST anomalies, and the January NPO index (SLP

difference between 20–30°N, 190–210°E and 55–65°N, 190–210°E, corresponding to the pattern in figure 2 (b) from 1958 to 2016 in figures 3(c)–(h). We confirm that the patterns of the SLP and SST anomalies at lag 0 and 2 months (bottom two panels) closely match the CEOF2 patterns shown in figure 2 and the evolution in 2014 (figures 1(a)–(c)). The NPO is strengthened initially, followed by the prominent pattern of SST anomalies through the development of the CEOF2. Similar correlations of the SLP anomalies persist until March (figure 3(g)). Thereafter, the SLP anomalies diminish gradually over time. Figure S5 further shows the lead–lag correlation between the North Pacific SST anomalies (blue box in figure 2(d)) and the NPO index. The largest correlation exists in February and March, consistent with the described pattern. The southern lobe of the NPO (figure S5(c)) actually plays a larger role than the northern lobe.

#### 4. Discussion

Two other super El Niño events have been observed in the last three decades (i.e. 1982/83 and 1997/98). Why, therefore, did we not see the extremely high and positive PC2 of CEOF2 (or a large warm Blob as the ocean signature) in these two El Niño events (figure 2 (e)) if it is a useful precursor? In fact, Ding *et al* (2015a) showed that the positive VM existed in both periods (their table 1), indicating the persistent impact of the VM on the El Niño (also seen as the positive and large PC2 in figure 2(e) before these super El Niños). However, the magnitude of the PC2 in those years was weaker than that of the most recent event. This is mainly because the defined CEOF2 only corresponds to the triggering and amplifying forcing from the NH. The other dominant ENSO amplifier results from the

influence of the Southern Hemisphere (SH) quadrupole SST anomaly patterns (similar to the extratropical VM impact in the North Pacific but with a different pattern) (Hong *et al* 2014, Zhang *et al* 2014, Ding *et al* 2015c). In 1997, the El Niño development was enhanced by warm subtropical SST anomalies associated with the SH quadrupole SST anomaly pattern so that the eastern tropical Pacific became warm enough to initiate the necessary O–A coupling in the central tropical Pacific (Ding *et al* 2015c). The SH extratropical impacts play a vital role in many canonical ENSO events (Zhang *et al* 2014, Ding *et al* 2015c). However, the SH subtropical SST anomalies in 2014 (Zhu *et al* 2016, Tseng *et al* 2017) provided unfavorable anomalous northeasterly wind conditions that hampered O–A coupling in the central–eastern tropical Pacific and were associated with reduced westerly wind bursts in the tropical Pacific (Menkes *et al* 2014). This led to the weak (or nearly neutral) El Niño at the end of 2014. The development of ENSO can be triggered from either NH or SH (Ding *et al* 2017). The development of a super El Niño requires both the VM and SH quadrupole SST anomaly patterns in the two hemispheres to support the continuous amplification of Bjerknes feedback in the tropics (e.g. as in 1982/83, 1997/98 and the El Niño after spring 2015).

We note that not all positive VM events lead to El Niños. Ding *et al* (2015a) found that over the period 1950–2011, ~30% of the positive VM events did not lead to ENSO development. But more than 80% of moderate to large ENSO events have the signature of positive (negative) VM prior to El Niño (La Niña), see table 1. The surface patterns associated with these VM events did not extend far enough toward the equator compared with those associated with other VM events related to ENSO. To initiate ENSO development, the preconditioned tropical subsurface heat content and its propagation are required to provide favorable tropical ocean conditions at interannual time scales (Chen *et al* 2015, Levine and McPhaden 2016, Tseng *et al* 2017). In terms of the 2015/16 El Niño, the warm water content was high from spring 2014 to early 2016 ([www.pmel.noaa.gov/el\\_nino/upper-ocean-heat-content-and-ens0](http://www.pmel.noaa.gov/el_nino/upper-ocean-heat-content-and-ens0)). This provides a favorable ocean condition for El Niño development. Therefore, both processes of O–A coupling and subsurface ocean temperature evolution are required to make these VM events effective in triggering warming from the central to eastern equatorial Pacific.

## 5. Conclusions

We showed that the warm Blob that developed in late 2013 and then decayed after late 2015 in the northeast Pacific was the ocean expression of the second O–A mode (CEOF2) variability in the tropical and North

Pacific (i.e. a part of the VM) and was an intermediate step leading to the 2015/16 El Niño. A neutral to weak El Niño condition was initially observed at the end of 2014, similar to the CEOF1 pattern but with weak magnitude (mainly due to the suppression of the SH subtropical impact). The heat content and SST anomalies in the tropical Pacific continuously evolved into a strong El Niño after April 2015 resulting from the re-intensification of the tropical–extratropical interaction, which reaches its mature phase at the end of 2015 with a robust CEOF1 pattern. With a weakened CEOF2 pattern in 2015/16 winter, the CEOF1 pattern (i.e. El Niño) decays dramatically in 2016.

Such CEOF2 patterns are frequently associated with the development/termination of an El Niño in the following winter/spring under certain conditions. The extremely large heat content accumulation in the tropics in 2014 (interannual time scale variation) intensifies the tropical–extratropical interaction (Di Lorenzo and Mantua 2016) so as to extend the 2015/16 El Niño longer than the previous El Niño events during the observational period (i.e. from the end of 2014 to early 2016). The 2015/16 El Niño differs from the previous large El Niño events in terms of the triggering hemisphere. Indeed, the basin-scale VM is still very clear in spring 2015 (not shown) but not the NPO dipole, thereby supporting the more direct connection of the VM than the NPO with ENSO variability. Here, the NPO only triggers the VM in late 2013, which favors the development of El Niño but does not guarantee its occurrence. However, throughout 2015, the El Niño develops fully through the positive Bjerknes feedback, leading a strong CEOF1-like pattern. These similarities confirm that the ENSO and the Blob are linked rather than independent phenomena. The record high recent warm Blob is a typical precursor to the strong 2015/16 El Niño. Our analysis does not focus on the causes of NPO variability, which require further model studies.

## Acknowledgments

We thank the two anonymous reviewers for their constructive comments that have helped to improve the clarity of the presentation. This study was supported by NSF Earth System Model (EaSM) grant 1419292 (EaSM-3: Collaborative Research: Quantifying Predictability Limits, Uncertainties, Mechanisms, and Regional Impacts of Pacific Decadal Climate Variability). Yu-heng Tseng is also supported by the MOST, Taiwan: project title ‘The development and validation of a new-generation, fully-coupled global climate system model’ (106-2111-M-002 -001). Xiaomeng Huang is supported in part by a grant from the State’s Key Project of Research and Development Plan (2016YFB0201100), and the National Natural Science Foundation of China (41375102).

## References

- Amaya D J, Bond N E, Miller A J and DeFlorio M J 2016 The evolution and known atmospheric forcing mechanisms behind the 2013–2015 North Pacific warm anomalies *US Clivar. Variat.* **14** 1–6
- Ashok K *et al* 2007 El Niño Modoki and its possible teleconnection *J. Geophys. Res.* **112** C11007
- Baxter S and Nigam S 2015 Key role of the North Pacific Oscillation–West Pacific Pattern in generating the extreme 2013/14 North American winter *J. Clim.* **28** 8109–17
- Bond N A, Overland J E, Spillane M and Stabeno P 2003 Recent shifts in the state of the North Pacific *Geophys. Res. Lett.* **30** 2183
- Bond N A, Cronin M F, Freeland H and Mantua N 2015 Causes and impacts of the 2014 warm anomaly in the NE Pacific *Geophys. Res. Lett.* **42** 3414–20
- Bretherton C S, Widmann M, Dymnikov V P, Wallace J M and Bladé I 1999 The effective number of spatial degrees of freedom of a time-varying field *J. Clim.* **12** 1990–2009
- Chang P *et al* 2007 Pacific meridional mode and El Niño—Southern Oscillation *Geophys. Res. Lett.* **34** L16608
- Chiang J C H and Vimont D J 2004 Analogous Pacific and Atlantic meridional modes of tropical atmosphere–ocean variability *J. Clim.* **17** 4143–58
- Chen H C, Sui C H, Tseng Y H and Huang H 2015 An analysis of the linkage of Pacific subtropical cells with the recharge–discharge processes in ENSO evolution *J. Clim.* **28** 3786–805
- Deser C *et al* 2012 ENSO and Pacific decadal variability in the community climate system model version 4 *J. Clim.* **25** 2622–51
- Di Lorenzo E *et al* 2008 North Pacific Gyre Oscillation links ocean climate and ecosystem change *Geophys. Res. Lett.* **35** L08607
- Di Lorenzo E *et al* 2015 ENSO and meridional modes: a null hypothesis for Pacific climate variability *Geophys. Res. Lett.* **42** 9440–8
- Di Lorenzo E and Mantua N 2016 Multi-year persistence of the 2014/15 North Pacific marine heatwave *Nat. Clim. Change* **6** 1042–7
- Ding R *et al* 2015a The Victoria mode in the North Pacific linking extratropical sea level pressure variations to ENSO *J. Geophys. Res. Atmos.* **120** 27–45
- Ding R *et al* 2015b Influence of the North Pacific Victoria mode on the Pacific ITCZ summer precipitation *J. Geophys. Res. Atmos.* **120** 964–79
- Ding R, Li J and Tseng Y H 2015c The impact of South Pacific extratropical forcing on ENSO and comparisons with the North Pacific *Clim. Dyn.* **44** 2017–34
- Ding R *et al* 2017 Joint impact of North and South Pacific extratropical atmospheric variability on the onset of ENSO events *J. Geophys. Res. Atmos.* **122** 279–98
- Feng J, Wu Z and Zou X 2014 Sea surface temperature anomalies off Baja California: a possible precursor of ENSO *J. Atmos. Sci.* **71** 1529–37
- Furtado J C, Lorenzo E D, Anderson B T and Schneider N 2012 Linkages between the North Pacific Oscillation and Central Tropical Pacific SSTs at low frequencies *Clim. Dyn.* **39** 2833–46
- Hartmann D L 2015 Pacific sea surface temperature and the winter of 2014 *Geophys. Res. Lett.* **42** 1894–902
- Hong L C, Lin Ho and Jin F F 2014 A Southern Hemisphere booster of super El Niño *Geophys. Res. Lett.* **41** 2142–9
- Huang B *et al* 2015 Extended Reconstructed Sea Surface Temperature version 4 (ERSST.v4). Part I: upgrades and intercomparisons *J. Clim.* **28** 911–30
- Jacox M *et al* 2016 Impacts of the 2015–2016 El Niño on the California current system: early assessment and comparison to past events *Geophys. Res. Lett.* **43** 7072–80
- Kay J E *et al* 2015 The Community Earth System Model (CESM) large ensemble project: a community resource for studying climate change in the presence of internal climate variability *Bull. Am. Meteor. Soc.* **96** 1333–49
- Kistler R *et al* 2001 The NCEP–NCAR 50-Year reanalysis: monthly means CD–ROM and documentation *Bull. Am. Meteor. Soc.* **82** 247–67
- Levine A F Z and McPhaden M J 2016 How the July 2014 easterly wind burst gave the 2015–2016 El Niño a head start *Geophys. Res. Lett.* **43** 6503–10
- Linkin M E and Nigam S 2008 The North Pacific Oscillation–West Pacific teleconnection pattern: mature-phase structure and winter impacts *J. Clim.* **21** 1979–97
- Menkes C E *et al* 2014 About the role of Westerly Wind Events in the possible development of an El Niño in 2014 *Geophys. Res. Lett.* **41** 6476–83
- Newman M *et al* 2016 The Pacific Decadal Oscillation, Revisited *J. Clim.* **29** 4399–427
- Tseng Y H, Hu Z Z, Ding R and Chen H C 2017 An ENSO prediction approach based on ocean conditions and ocean–atmosphere coupling *Clim. Dyn.* **48** 2025–44
- Vimont D J, Wallace J M and Battisti D S 2003 The seasonal footprinting mechanism in the Pacific: implications for ENSO *J. Clim.* **16** 2668–75
- Zhang Y, Wallace J M and Battisti D S 1997 ENSO-like interdecadal variability: 1900–93 *J. Clim.* **10** 1004–20
- Zhang H, Clement A and Di Nezio P 2014 The South Pacific Meridional Mode: a mechanism for ENSO-like variability *J. Clim.* **10** 769–83
- Zhu J *et al* 2016 The role of off-equatorial surface temperature anomalies in the 2014 El Niño prediction *Sci. Rep.* **6** 19677